Electronic and optical properties of three phases of titanium dioxide: Rutile, anatase, and brookite

Shang-Di Mo and W. Y. Ching
Department of Physics, University of Missouri–Kansas City, Kansas City, Missouri 64110
(Received 11 November 1994)

Using the self-consistent orthogonalized linear-combination-of-atomic-orbitals method in the local-density approximation, the electronic structure and the optical properties of three phases of titanium dioxide have been studied. For rutile, the calculated band structure, equilibrium lattice constant, and bulk modulus are in good agreement with other recent calculations and with experimental data. The results on the ground-state properties of anatase and brookite are reported. Compared with the rutile phase, anatase has similar ground-state properties except for a larger band gap, whereas brookite has relatively smaller bulk modulus. The optical properties of these three phases are also calculated using the band-structure results and compared with the available measurements. For the rutile phase, the anisotropic properties of the dielectric function are in good agreement with the reflectance spectroscopy. For the anatase phase, there are very limited experimental optical data for comparison. For the brookite phase, no experimental data are available. Our calculations show subtle differences in the optical properties of these three phases.

I. INTRODUCTION

Titanium dioxide (TiO_2) forms three distinct polymorphs: rutile, anatase, and brookite. For the past several decades, TiO_2 has been extensively studied for its interesting electric,[1,2] magnetic,[3] catalytic,[4] and electrochemical properties.[5] Based upon these properties, a variety of technological applications are possible. TiO_2 has been widely used in catalysis, in electrochromism, and as sensors.[6] It has also been used as pigmentation for paints and polymers. In particular, since about 1971, when Fujishima and Honda reported their work on a photoelectrochemical cell possessing an anode of TiO_2,[7] photocatalysis has developed into a major area of intensive investigation. From that time on, TiO_2 has continued to hold a dominant position in photocatalysis.[8]

There have been many studies of the electronic and structural properties of TiO_2, both of experimental[9–16] and theoretical aspects.[17–28] However, only the rutile phase has been studied extensively. The main reason is that most crystal-growth techniques basically yield TiO_2 in the rutile phase. Also, rutile has the simplest and best known structure. On the experimental side, the electronic structure of rutile TiO_2 has been studied by various techniques such as ultraviolet photoemission spectroscopy (UPS),[9,10] x-ray emission spectroscopy,[11] x-ray photoemission spectroscopy (XPS),[12,13] electron-energy-loss spectroscopy (EELS),[14,15] and Auger-electron spectroscopy (AES).[16] Theoretical studies reported so far are the linear muffin-tin orbital (LMTO) calculation of Poumellect, Durham, and Guo,[17] and those using an empirical tight-binding method.[18,19] Cluster methods[20,21] have also been applied to calculate the electronic structure of rutile. Recently, a detailed study of the structural, electronic, and optical properties of rutile has been carried out by Glassford and Chelikowsky.[22] They used *ab initio* soft-core pseudopotentials constructed according to the local-density approximation (LDA) theory and a plane-wave basis, and obtained results in very good agreement with experiments. They followed up with an *ab initio* calculation of Ru-doped TiO_2, and suggested that there are Ru-induced defect states within the fundamental band gap.[23] This is consistent with absorption and photoelectrochemical experiments.[29,30] Very recently, *ab initio* full-potential linearized-augmented-plane-wave (LAPW) method was used to calculate the electronic structure and geometry of a clean TiO_2 [110] rutile face.[24] Surface-induced states were also obtained. The discrete variational $X\alpha$ (DV-$X\alpha$) cluster method has been used by one of us to calculate impurity states in transition-metal-doped rutile.[25] In an earlier paper by Hally, Michalewicz, and Tit, electronic structure of multiple vacancies in rutile TiO_2 was studied by the equation-of-motion method in conjunction with a tight-binding model.[26]

In contrast to the rutile phase, there are few theoretical investigations of the anatase phase.[27,28] Pseudopotential Hartree-Fock and extended Hückel tight-binding (EHT) calculations were carried out for the anatase phase. The former predicted a much larger band-gap value, while the latter supplied an estimation of equilibrium bond distances in anatase by a total-energy minimum search. For brookite, to the best of our knowledge, no theoretical study of the electronic and optical properties has been reported so far. This is probably due to the difficulty in the calculation caused by the larger number of atoms in the unit cell of these two phases.

Actually, anatase and brookite have also attracted a great deal of interest in connection with technological applications.[31,32] Both rutile and anatase were intensively studied for photocatalysis and photoelectrochemical applications, but anatase is the phase more actively investigated. It has been pointed out that the Fermi level in anatase is higher than that of rutile by about 0.1 eV.[33] It is also known that anatase plays a key role in the injection process of photochemical solar cells with high con-

0163-1829/95/51(19)/13023(10)/$06.00

version efficiency.[32] Moreover, it has been reported that anatase thin film has different electrical and optical properties from the rutile film.[34] The essential difference is that anatase thin film appears to have a wider optical-absorption gap and a smaller electron effective mass, resulting in a higher mobility for the charge carriers. These properties are beneficial to further applications in optoelectronic and other devices. It is therefore necessary to have a systematic theoretical investigation on the electronic and optical properties of all three phases of TiO_2.

In this paper, we present the results of a detailed study of the electronic structure and optical properties of rutile, anatase, and brookite using the first-principles orthogonalized linear-combinations-of-atomic-orbitals (OLCAO) method. We organize our paper as follows. In Sec. II, we briefly describe the theoretical method and the procedure of calculation. We then describe the crystal structure information for the three phases in Sec. III. Section IV contains the main results of the electronic structure, ground-state, and optical properties of the three phases. We also discuss our results in comparison with other existing calculations and experimental data. In Sec. V, a brief summary and some conclusions are given.

II. METHOD AND PROCEDURE OF CALCULATION

We use the first-principles self-consistent OLCAO method to calculate the electronic structure of TiO_2. Since this method has been described in detail,[35] we merely outline the essential procedures involved in the present calculation.

The Bloch functions in the band-structure calculation are constructed from the linear combination of atomic orbitals which are represented by a linear combination of a set of Gaussian-type orbitals (GTO's). In the present case, a full basis set consisting of atomic orbitals of O ($1s$, $2s$, $2p_x$, $2p_y$, $2p_z$, $3s$, $3p_x$, $3p_y$, and $3p_z$) and Ti ($1s$, $2s$, $2p_x$, $2P_y$, $2p_z$, $3s$, $3p_x$, $3p_y$, $3p_z$, $3d_{xy}$, $3d_{yz}$, $3d_{zx}$, $3d_{x^2-y^2}$, $3d_{3z^2-r^2}$, $4s$, $4p_x$, $4p_y$, $4p_z$, $5s$, $5p_x$, $5p_y$, $5p_z$, $4d_{xy}$, $4d_{yz}$, $4d_{zx}$, $4d_{x^2-y^2}$, and $4d_{3z^2-r^2}$) is chosen. Each atomic orbital has GTO's with exponentials ranging from 0.15 to 50 000. The inclusion of extra atomic orbitals corresponding to excited states in the full basis set is necessary in order to provide additional variational freedom.

In the present study, we adopted a procedure of basis optimization. The initial atomiclike wave functions in the basis set are obtained by solving the free-atom problem self-consistently within the local-density-approximation (LDA) scheme. After the crystal calculation, the self-consistent potential is expressed in the form of site-decomposed atomiclike potentials.[35] Sets of atomiclike orbitals for each atom are then obtained using a single Gaussian contraction on the site-decomposed atomiclike potentials which contain the effect of the crystalline environment. The self-consistent crystalline calculation is then repeated with the contracted orbitals in the basis set. The procedure repeats until the difference between the old and new orbital basis becomes quite small. In the present calculation, the convergence in basis optimization is achieved in only two cycles. For the TiO_2 system, the hybridization between the O_{2p} and Ti_{3d} orbitals is very strong. In some sense, the electronic properties of TiO_2 depend largely on the accurate representation of the O_{2p} and Ti_{3d} orbitals. This is particularly important in the gap region where the range of interaction of Ti_{3d} and O_{2p} orbitals strongly influence the gap size. As a result of basis optimization, it is found that the fundamental LDA energy gap of rutile is slightly increased from the value with a nonoptimized calculation, in better agreement with experiment. The same optimized basis is used for the other two TiO_2 phases since there is no fundamental difference in the bonding between Ti and O among the three phases.

The total crystal potential is constructed according to the LDA prescription to set up the one-electron Kohn-Sham equation, with the Wigner interpolation formula[36] used to account for correlation effect. The potential and charge-density functions in the OLCAO method are expressed as sums of atom-centered Gaussian functions with fixed exponentials. We adopt 18 Gaussians per Ti-centered function with exponentials ranging from 0.18 to 100 000 and 16 Gaussians per O-centered function with exponentials ranging from 0.16 to 100 000. The coefficients of the charge-density expansion are obtained by a numerical fitting procedure. The fitting accuracy in which the deviations of less than 0.001–0.004 electrons per valence electron are achieved for the three TiO_2 phases. Past experience indicates that this level of fitting accuracy is very adequate for band-structure and optical properties calculations.

In the self-consistent iterations, the number of special **k** points used in the irreducible portion of the Brillouin zone (BZ) ranges from 4 to 8 for the three TiO_2 phases. Self-consistency in the potential is generally achieved in less than 20 iterations in which the energy eigenvalues change by less than 0.0001 eV. For the density of states (DOS) and optical calculations, a much larger number of regularly spaced **k** points are used (93, 88, and 72 in the irreducible parts of the BZ for rutile, anatase, and brookite, respectively). The DOS and the optical conductivities are evaluated by using the linear analytic tetrahedron method.[37] The partial DOS (PDOS) are obtained according to the Mulliken partitioning scheme.[38] It is understood that PDOS obtained this are only approximate, especially with a full basis set used in the calculation.

For the total-energy calculation, we assume that the lattice ratios and internal parameters of the three crystals are fixed, and evaluate the total energy E as a function of the change in the volume fraction V/V_0, where V_0 is the experimental volume. Using the calculated E versus V/V_0 data, we evaluate the bulk static properties by fitting the calculated data to Murnaghan's equation of states.[39] The theoretical minimum volume $V_{\min}$, the bulk modulus B, and the pressure coefficient B' are obtained. For the rutile phase, we did additional calculations on the total energy E by varying the c/a ratio and the internal parameter u while fixing volume at V_0. Through this two-dimensional energy minimum search, an E versus c/a and u contour map is obtained. Based on this map, the theoretically predicted lattice parameters c/a and u are determined.

For optical properties calculation, the momentum matrix elements between each pair of the occupied valence band (VB) and the empty conduction band (CB) are calculated at regularly spaced **k** points using the *ab initio* crystal wave function. The frequency-dependent interband optical conductivity in the dipole approximation is then evaluated by considering all possible pairs of **k**-conserving transitions.[35] The imaginary part of the dielectric function $\varepsilon_2(\omega)$ is related to the interband optical conductivity $\sigma_1(\omega)$ through $\varepsilon_2(\omega)=(4\pi/\omega)\sigma_1(\omega)$. The real part $\varepsilon_1(\omega)$ can be obtained numerically by the Kramers-Kronig transformation. The zero-frequency limit of $\varepsilon_1(\omega)$ gives the electronic part of the static dielectric constant ε_0. The electron-energy-loss function (ELF) is obtained from $-\mathrm{Im}[1/(\varepsilon_1+i\varepsilon_2)]$.

III. CRYSTAL STRUCTURES

TiO_2 occurs in three crystalline polymorphs: rutile, anatase, and brookite. The basic unit-cell structures of these phases are shown in Fig. 1. The crystal parameters, the Ti-O interatomic distances, and the O—Ti—O bond angles for the three phases are summarized in Table I. Rutile and anatase are both tetragonal, containing six and 12 atoms per unit cell, respectively. In both structures, each Ti atom is coordinated to six O atoms and each O atom is coordinated to three Ti atoms. In each case, the TiO_6 octahedron is slightly distorted, with two Ti—O bonds slightly greater than the other four, and with some of the O—Ti—O bond angles deviating from 90°. The distortion is greater in anatase than in rutile. The structure of rutile and anatase crystals has been described frequently in terms of chains of TiO_6 octahedra having common edges.[40] Two and four edges are shared in rutile and anatase, respectively.

The third form of TiO_2, brookite shown in Fig. 1(c), has a more complicated structure. It has eight formula units in the orthorhombic cell. The interatomic distances and the O—Ti—O bond angles are similar to those of rutile and anatase. The essential difference is that there are six different Ti—O bonds ranging from 1.87 to 2.04 Å. Accordingly, there are 12 different O—Ti—O bond angles ranging from 77° to 105°. In contrast, there are only two kinds of Ti—O bonds and O—Ti—O bond angles in rutile and anatase. We can also envision brookite as formed by joining together the distorted TiO_6 octahedra sharing three edges.[41]

TABLE I. Crystal structure data of TiO_2.

	Rutile[a]	Anatase[a]	Brookite[b]
Crystal structure	tetragonal	tetragonal	orthorhombic
Lattice constants (Å)	$a=4.5936$	$a=3.784$	$a=9.184$
	$c=2.9587$	$c=9.515$	$b=5.447$
			$c=5.145$
Space group	$P4_2/mnm$	$I4_1/amd$	$Pbca$
Molecule/cell	2	4	8
Volume/molecule (Å^3)	31.2160	34.061	32.172
Density (g/cm^3)	4.13	3.79	3.99
Ti—O bond length (Å)	1.949(4) 1.980(2)	1.937(4) 1.965(2)	1.87∼2.04
O—Ti—O bond angle	81.2° 90.0°	77.7° 92.6°	77.0°∼105°

[a]Reference 40.
[b]Reference 41.

IV. RESULTS AND DISCUSSION

A. Band structure and density of states

The calculated band structures along the symmetry lines of the BZ for rutile, anatase, and brookite are shown in Fig. 2. The corresponding DOS and PDOS are presented in Fig. 3.

For rutile, the calculated band gap of 1.78 eV is direct at Γ, smaller than the reported experimental gap of 3.0 eV,[42] and close to other recent calculations.[17,22,43] This is expected for the LDA calculation which generally underestimates the experimental band gap for insulators and semiconductors. The $X\alpha$ cluster calculation[44] gives a large gap of 3.89 eV which has to do with the finite number of discrete energy levels in cluster-type calculations rather than being a reflection of better agreement with

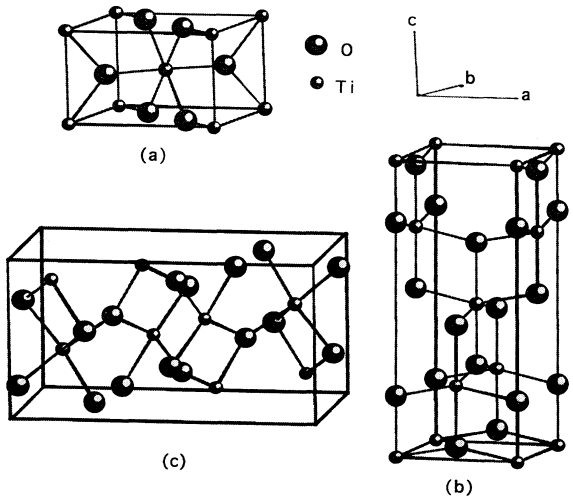

FIG. 1. Crystal structures of TiO_2. (a) Rutile. (b) Anatase. (c) Brookite.

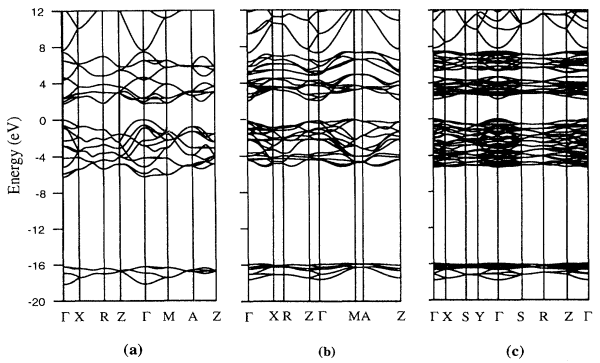

FIG. 2. Calculated band structures of rutile (left panel), anatase (middle panel), and brookite (right panel).

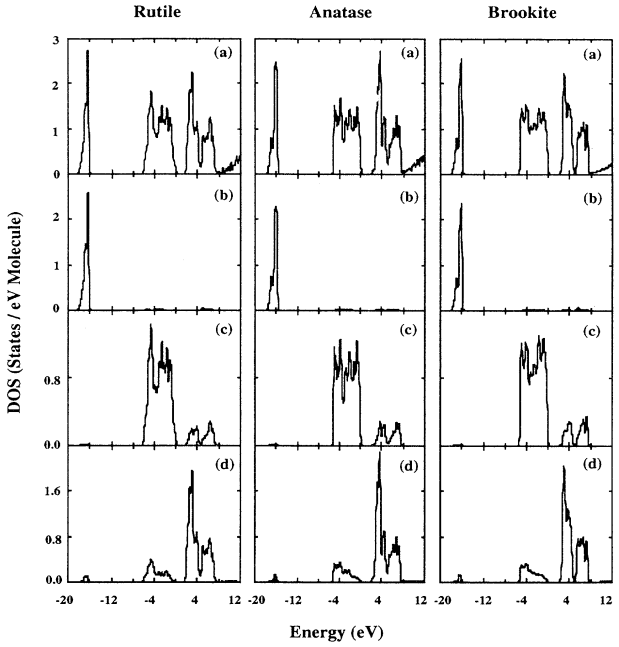

FIG. 3. Calculated total and partial DOS's of rutile (left panel), anatase (middle panel), and brookite (right panel): (a) total, (b) O_{2s}, (c) O_{2p}, and (d) Ti_{3d}.

experiment. The upper valence band is composed of O_{2p} orbitals and has a width of 6.22 eV. The lower O_{2s} band is 1.94 eV wide. These numbers are in good agreement with experimental values of 5.4 and 1.9 eV,[45] respectively. The separation energy between O_{2s} valence states and the minimum of the conduction band (CB) is 17.98 eV, which is in line with the other calculated values of 17.0 eV (Ref. 22) and 17.3 eV,[43] and the experimental Auger spectroscopy value of 16–18 eV.[16] The lowest conduction band consists of two sets of Ti_{3d} bands and has a width of 5.9 eV. These two sets of bands have their atomic origin from the hybridized states of t_{2g} and e_g. The above band-structure features are also evident in the DOS diagram. Kowalczyk[45] reported an energy separation of 1.9 eV between the two major features in the valence band. Such a double-peak structure is quite evident in our calculated total DOS in Fig. 3(a) for rutile. This double-peak structure has its origin in the separation between the nonbonding and bonding O_{2p} states. A similar two-peak feature is also found in the CB. The two distinct CB parts have widths of 2.6 and 3.3 eV. Glassford and Chelikowsky[22] and also Sorantin and Schwarz[43] attributed this feature as due to crystal-field splitting of the Ti_{3d} band states. Their calculated widths for these CB's are 2.9 and 3.3 eV and 2.6 and 2.9 eV, respectively. Our calculated Ti_{3d} DOS in Fig. 3(d) for rutile shows that the separation between the centroids of the two peaks in the CB is about 2.7 eV. This is in close agreement with the experimental peak spacings of 2.5 eV from EELS for the Ti L_3 and O K data.[15] A similar measurement of Ti K-edge data by Tsutsumi[11] gives a peak separation of roughly 3 eV. The PDOS also suggest that there is a substantial degree of hybridization between O_{2p} and Ti_{3d} in both the CB and VB regions, indicating strong interactions between Ti and O atoms in rutile. It also means that the excitation across the band gap involves both O_{2p} and Ti_{3d} states.

Unlike rutile, the calculated minimal band gap of 2.04 eV for anatase is indirect. The bottom of the CB is at Γ and the top of the VB is at M. However, the energy at Γ is only 0.18 eV lower than the top of the VB. Thus we can still regard anatase as a direct-gap insulator. The reported experimental gap value of 3.2 eV for anatase[46] is 0.2 eV larger than that of rutile. This is consistent with our calculation, which shows the gap for anatase is larger than that of rutile by 0.26 eV. Our calculation also shows the upper VB width of anatase (5.17 eV) is less than that of rutile by about 1 eV. The lower O_{2s} band of 1.76 eV wide is also narrower than that of rutile, and lies 17.88 eV below the CB minimum. The general features of the VB for anatase are quite similar to rutile. Comparing the DOS of anatase shown in Fig. 3 with that of rutile, the only difference appears to be that the double-peak feature is less distinct, especially for the lower peak. The only XPS result for anatase[47] indicates that the VB of anatase has a width of 4.75 eV. There is also a two-peak structure in the VBS with a separation energy of 2.0 eV. These features are all in good agreement with our calculated values.

We are not aware of any reported experimental data for brookite. However, we expect the electronic structure of brookite to be similar to that of anatase because there is only minor differences in the local crystal environment between the two phases. Our calculation shows that brookite also has a direct band gap of 2.20 eV at Γ, which is larger than both rutile and anatase. The upper VB has a total width of about 5.31 eV, which is close to that of anatase. The width of the lower O_{2s} band of 1.85 eV is also close to that of anatase. The calculated results on the band structures for the three phases of TiO_2 are summarized in Table II.

B. Total-energy calculation

We have calculated the total energies for three phases of TiO_2 as a function of their crystal volume within the LDA of the density-functional theory. Figure 4 shows the total energy E versus V/V_0 curves for the three phases were V_0 is the reported experimental equilibrium volume. We have assumed a uniform scaling of the lattice constants with a fixed c/a ratio, and calculated the total energy as a function of volume. For each phase, both the actual data points and the fitted curve to Murnaghan's equation of state[39] are presented. The zero energy per molecule for each curve is set at the calculated minimum. The bulk properties obtained from the total-energy calculations and some available experimental data are listed in Table III.

For rutile, the calculated equilibrium volume is within 2% of the experimental value. We also obtain the bulk modulus B and the pressure coefficient B' to be 209 GPa and 6.11, respectively. These are in excellent agreement with the experimental values of 216 GPa and 6.76.[48] Glassford and Chelikowsky obtained the values of B and B' to be 240 GPa and 4.63. We should mention that the

TABLE II. Calculated band structure of TiO_2. *O*: Direct gap (Γ). ID: Indirect gap ($\Gamma \rightarrow M$).

	Rutile	Anatase	Brookite
Band gap (eV)			
Calc. (present)	1.78(*D*)	2.04(ID) 2.22(*D*)	2.20(*D*)
(others)	2.0,[b]1.5[c],3.89[d]		
Experiment	3.0[c]		
Upper VB width (eV)			
Calc. (present)	6.22	5.17	5.31
(others)	5.0,[d,c]5.7[b]		
Experiment	5.4[f]	4.75[g]	
O_{2s} bandwidth (eV)			
Calc. (present)	1.94	1.76	1.85
(others)	1.8,[c]1.9[d]		
Experiment	1.9[f]		
Gap between O_{2s} bands and minimum of CB (eV)			
Calc. (present)	17.98	17.88	18.16
(others)	17.0,[b]17.3[c]		
Experiment	16–18[h]		

[a]Reference 17.
[b]Reference 22.
[c]Reference 43.
[d]Reference 44.
[e]Reference 42.
[f]Reference 45.
[g]Reference 47.
[h]Reference 16.

B value depends to some extent on the choice of the equation of states. The pressure coefficient B' is naturally less accurate than *B* both experimentally and theoretically.

Fixing the unit-cell volume of rutile at the calculated minimum, we also explore the variations of total energy with the c/a ratio, and the internal parameter u which determines the atomic positions within the unit cell. The result is shown as a contour map in the inset of Fig. 4. Our calculation predicts the c/a and u values in rutile to be 0.6454 and 0.3043, respectively. These values are in excellent agreement with the measured values of 0.6441 and 0.3408.[41] Up to now, there were three attempts to determine the structural parameter u in rutile minimizing the total energy while fixing the volume and the c/a ratio. The calculated u values are 0.305 (Ref. 22), 0.3064 (Ref. 43), and 0.297 (Ref. 49), respectively. However, since the relationship between the structural parameters is not explicit, we conclude that our calculated values obtained from a two-dimensional energy surface to be more reliable.

As listed in Table III, the calculated equilibrium volumes for anatase and brookite are also very reasonable. For anatase, our calculated V_{min} is larger than the experimental V_0 by more than 3%. For brookite, the difference between the predicted volume and the measured volume is less than 0.1%. This excellent agreement is probably fortuitous. It is found that anatase has a bulk modulus of 272 GPa, which is larger than that of rutile by 30%. On the other hand, the bulk modulus of brookite is presented to be only 137 GPa, almost one half of anatase's. That means brookite is a much more soft material than anatase and rutile. This apparent softness in the brookite phase is a bit surprising, but is probably due to the more distorted nature of the TiO_6 octahedron in

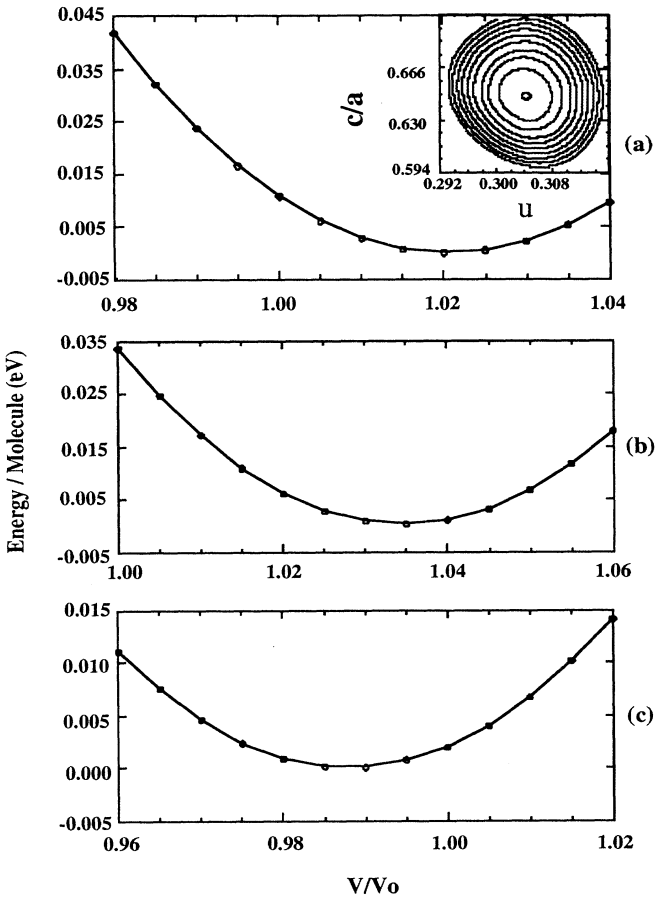

FIG. 4. Calculated total energies of (a) rutile, (b) anatase, and (c) brookite vs crystal volume. Inset: Energy contours with the variation of c/a ratio and internal parameter u.

TABLE III. Calculated equilibrium properties of TiO_2. The experimental value is in parentheses. V_0 is the experimental cell volume, and V_{min} is the calculated cell volume corresponding to a minimum in the total energy. For anatase and brookite, experimental values of c/a and u are used.

	Rutile	Anatase	Brookite
V_{min}/V_0	1.021	1.035	0.99
c/a ratio			
Present work	0.6454(0.6441[a])		
others	0.637[b]		
u parameter			
Present work	0.3043 (0.3048[a])		
others	0.305,[b]0.3064,[c]0.297[d]		
B (GPa)			
Present work	209.34 (216.0[e])	272.11	137.32
others	240.0[b]		
B'			
Present work	6.11 (6.76[e])		
others	4.63[b]		

[a]Reference 40.
[b]Reference 22.
[c]Reference 43.
[d]Reference 49.
[e]Reference 48.

brookite. As shown in Table I, the Ti—O bonds in brookite vary from 1.87 to 2.04 Å and the O—Ti—O bond angles from 77° to 105°. In a highly ordered structure such as in rutile or anatase, TiO_6 will be a more rigid structural unit under an isotropic compression. We are unable to locate any experimental bulk modulus measurement for anatase or brookite so far. Further experimental work is highly desirable.

C. Optical properties

In spite of numerous experimental and theoretical studies of the electronic structure of rutile in recent years, there is only one detailed theoretical investigation of its optical properties.[22] The work of Ref. 22 shows excellent agreement between the theoretical calculation and experimental data.[50,51] Recently, some limited optical data for anatase have emerged.[52] For brookite, no existing experimental or theoretical works can be located.

In this section, we shall present our results of first-principles optical calculations for the three TiO_2 phases. The calculated real and imaginary parts of the dielectric functions for the three phases of TiO_2 up to a photon energy of 12 eV are shown in Fig. 5. In order to study optical anisotropy in TiO_2, we resolve the imaginary parts of the dielectric functions into two components for rutile and anatase which have tetragonal unit cells: the in-plane component $\varepsilon_{2xy}(\omega)$ which is the average over the x and the y components, and the perpendicular or the z component $\varepsilon_{2z}(\omega)$. These are shown in Figs. 6 and 7, respectively. For brookite, which is orthorhombic, we simply resolve $\varepsilon_2(\omega)$ into three Cartesian components which are shown in Fig. 8.

For rutile, the fundamental absorption edge in $\varepsilon_{2xy}(\omega)$

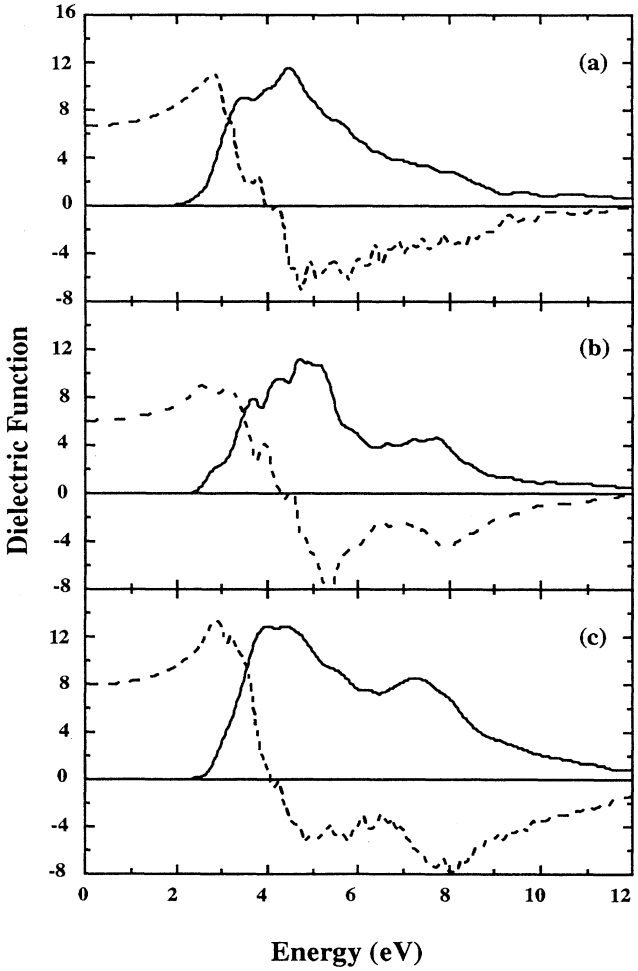

FIG. 5. Calculated imaginary parts (solid line) and real parts (dashed line) of the dielectric functions of TiO_2: (a) rutile, (b) anatase, and (c) brookite.

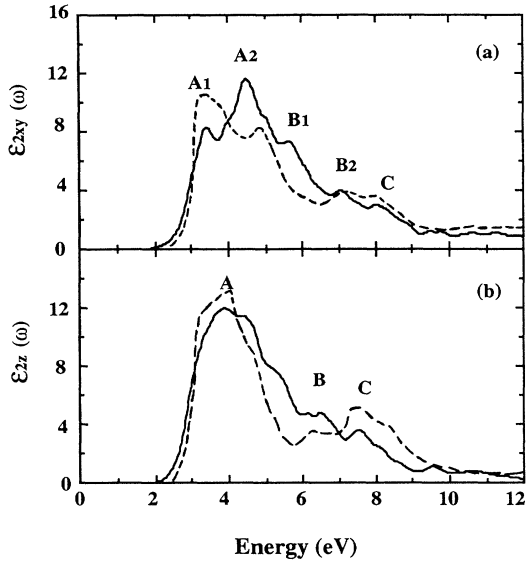

FIG. 6. Anisotropic components of $\varepsilon_2(\omega)$ of rutile: (a) perpendicular component of $\varepsilon_{2xy}(\omega)$; (b) parallel component of $\varepsilon_{2z}(\omega)$. The dashed lines are calculated results of Ref. 22.

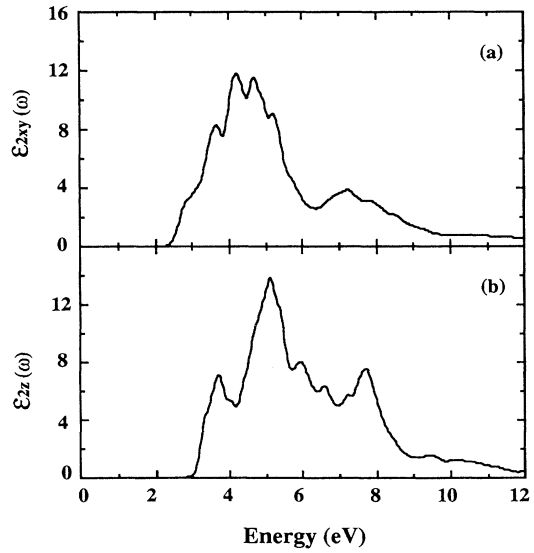

FIG. 7. Anisotropic components of $\varepsilon_2(\omega)$ of anatase: (a) perpendicular component of $\varepsilon_{2xy}(\omega)$; (b) parallel component of $\varepsilon_{2z}(\omega)$.

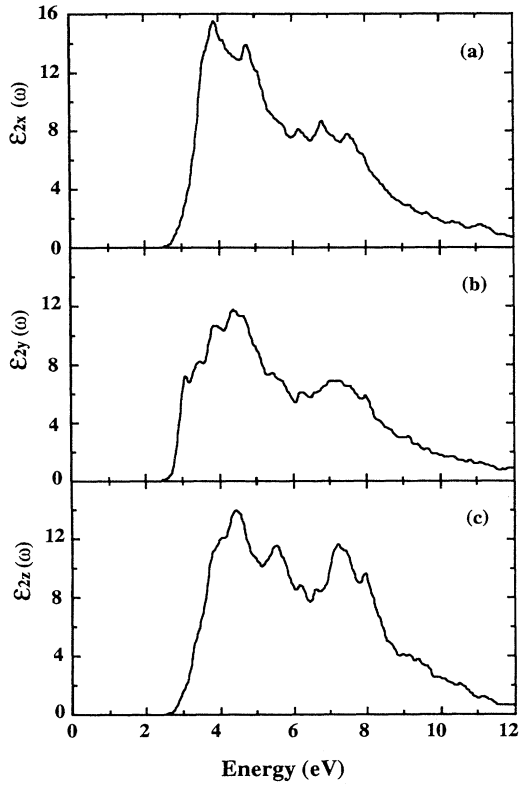

FIG. 8. Cartesian components of $\varepsilon_2(\omega)$ for brookite: (a) $\varepsilon_x(\omega)$, (b) $\varepsilon_y(\omega)$, and (c) $\varepsilon_y(\omega)$.

occurs at 1.82 eV, resulting from the interband transitions between the topmost VB and the bottom of the CB. Beyond the absorption edge, the experimental data[50] show five major peaks at 4.00, 5.35, 6.10, 7.40, and 8.05 eV. As shown in Fig. 6(a), our calculated $\varepsilon_{2xy}(\omega)$ curve reproduces these features quite well, with peak structures located at 3.47, 4.50, 5.71, 7.07, and 8.09 eV. Our results also in fair agreement with the calculation of Glassford and Chelikowsky.[22] A detailed comparison of the positions of the structures between the present calculation and experimental data as well as other theoretical results is shown in Table IV. The general agreement is reasonable. For the component $\varepsilon_{2z}(\omega)$, the absorption edge occurs at a slightly larger value 1.97 eV compared to the $\varepsilon_{2xy}(\omega)$ component. The experimental curve for the perpendicular component shows three peaks at 4.11, 6.63, and 7.87 eV. These features are again well reproduced by the present calculation, as shown in Fig. 6(b). Our calculated $\varepsilon_{2z}(\omega)$ curve also shows three peaks at 3.93, 6.50, and 7.53 eV. Also shown are the calculated data of Ref. 22. In principle, one can obtain the optical reflectivity spectrum $R(\omega)$ from the calculated dielectric function and compare with experimental data of Ref. 52. We find our converted $R(\omega)$ curve in the higher-energy range (>6.0 eV) to be less satisfactory, although appropriate structures can still be identified. Part of the reason may be due to the inaccuracy in the $\varepsilon_1(\omega)$ curve in this range by Kramers-Kronig conversion.

As shown in Fig. 5, the $\varepsilon_2(\omega)$ curves of anatase and brookite have similar general features to those of the rutile phase. The threshold energies for anatase and brookite are 2.27 and 2.22 eV, respectively. These are consistent with their corresponding direct-band-gap values. It is not meaningful to fully analyze the peak structures in the $\varepsilon_2(\omega)$ curves for anatase and brookite because detailed experimental data are not available. Still, we can identify two similar major-peak structures for anatase and brookite, which are at 4.78 and 7.73 eV and 4.19 and 7.34 eV, respectively. In each case, the lower main peaks result from the transitions between the O_{2p} orbitals and the t_{2g} conduction-band states, while the higher peak result from transitions between the O_{2p} orbitals and the e_g conduction-band states. There is a substantial optical anisotropy in the dielectric functions for anatase and brookite, as shown in Figs. 7 and 8, respectively.

Figure 5 also shows the real part of the dielectric functions for the three phases of TiO_2 which are obtained from $\varepsilon_2(\omega)$ by the Kramers-Kronig transformation. All three curves have very similar features in the long-wavelength limit ($\lambda \rightarrow \infty$), which are expected. The most important information is the value of $\varepsilon_1(\omega)$ in the limit of zero frequency. This corresponds to the electronic part of the static dielectric constant of the material. Our calculated values of ε_0 are 6.62 and 6.04 for rutile and anatase. These agree reasonably well with the measured values of 6.33 and 5.62 for rutile and anatase,[53] respectively. The perpendicular and parallel components of ε_0 for rutile are also in fairly good agreement with the values obtained from the reflectance measurement[50] and other theoretical values.[22] These values are listed in Table V. For brookite, we predict a much larger static dielectric constant of 7.89 compared with the other two phases. In general, our calculated values are somewhat larger than the experimental results. This is partly due to the underestimation of the fundamental band gaps for calculations based on the LDA theory.

It is interesting to investigate the optical transitions in TiO_2 at a higher photon energy. We thus extend our cal-

TABLE IV. Comparison of structures in the calculated imaginary part of the dielectric function of rutile with experimental data (Ref. 50) and other first-principles results (Ref. 22) (units in eV).

$\varepsilon_{2xy}(\omega)$	Present work	Experiment	Ref. 22	$\varepsilon_z(\omega)$	Present work	Experiment	Ref. 22
A_1	3.47	4.00	3.06	A	3.93	4.11	3.06
A_2	4.50	5.35	4.67				
B_1	5.71	6.10	6.06	B	6.50	6.63	6.15
B_2	7.07	7.40	6.96				
C	8.09	8.05	7.59	C	7.53	7.87	7.27

TABLE V. Calculated static dielectric constants of TiO_2.

	Rutile	Anatase	Brookite
Static dielectric constant $\varepsilon(0)$			
Calc. (present)	6.62	6.04	7.89
Experiment	6.33[a]	5.62[a]	
Components:			
$\varepsilon_x(0)$			8.34
$\varepsilon_y(0)$			7.21
$\varepsilon_{x-y}(0)$	6.46, 6.4,[b] 5.80[c]	5.99	
$\varepsilon_z(0)$	6.95, 7.3,[b] 7.07[c]	6.13	8.13

[a]Reference 53.
[b]Reference 22.
[c]Reference 50.

culation to 20 eV of photon energy and analyze the energy-loss functions (ELF's) which are obtained as $I_{\mathrm{ELF}} = -\mathrm{Im}(1/\varepsilon(\omega))$. The results are shown in Fig. 9. Generally speaking, the most prominent peak in the ELF spectrum is identified as the plasmon peak. The peak position, or the plasma frequency ω_p, signals the frequency of collective excitation of the electronic charge density in the crystal. It appears that there are three plasmon peaks (at 10.4, 12.0, and 13.9 eV) in rutile. In contrast to rutile, anatase and brookite have only one major plasma peak located at 12.7 and 19.5 eV, respectively, within the 20-eV range. We also note that the general features of the energy-loss functions of rutile and anatase are very similar, but that of brookite shows a significant difference, especially in the shifting of ω_p to higher energy.

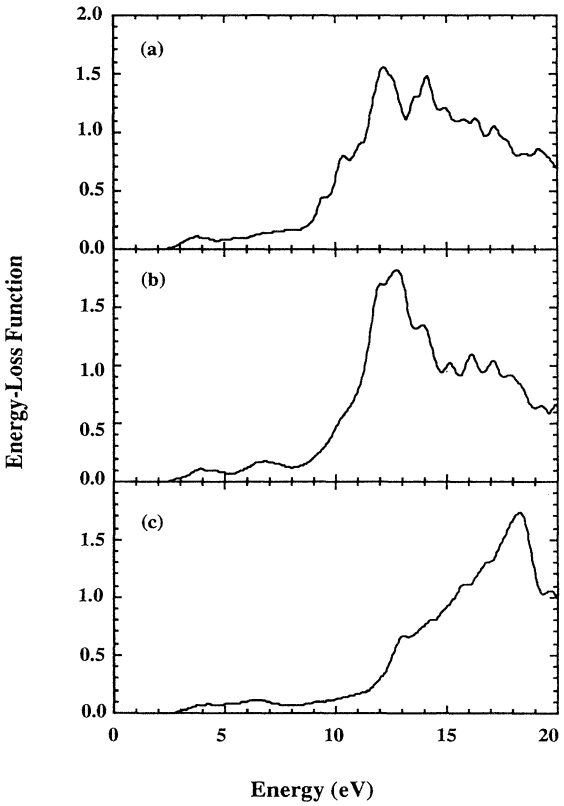

FIG. 9. Calculated energy-loss functions for (a) rutile, (b) anatase, and (c) brookite.

V. SUMMARY AND CONCLUSIONS

We have presented results of first-principles OLCAO studies of the electronic and optical properties of three phases of TiO_2. The electronic structures of all three TiO_2 phases have been studied. In particular, a basis optimization procedure has been implemented in the present calculation. For ground-state properties, a number of important electronic parameters such as bandwidths, band gaps, and densities of states have been obtained. Except for the band-gap values, the electronic parameters for the three phases are similar. Rutile has the smallest band gap of 1.78 eV (direct), while brookite has the largest direct band gap of 2.20 eV. The minimum band gap for anatase is indirect with a value of 2.04 eV. Our calculated results are consistent with experimental data and a few other recent calculations.

The present calculation is based on the density-functional theory in its local approximation, which is strictly valid only for the ground state. It is well known that this results in an underestimation of band gaps for semiconductors and insulators, because a single exchange-correlation potential is inadequate for an insulating system where the exchange-correlation potential is likely to be discontinuous across the gap.[54,55] Generally speaking, there are two approaches to enlarge the band gap. One is to apply the self-interaction correction (SIC).[56] In this model, the unphysical self-interaction in the Hartree term is removed by an orbital-by-orbital correction to the exchange-correlation potential. The SIC for insulators is generally applied to the VB only, and can significantly improve the gap values in large gap insulators.[56–58] The other approach is to go beyond the density-functional theory, and use a Green's-function formalism to study the self-energy term of quasiparticles in the many-particle system. This approach has been quite successful, especially in semiconductors.[59–63] A simplified version for self-energy correction based on a two-band Sterne-Inkson model[64] has been implemented in the OLCAO method, and gives satisfactory results for several semiconductor crystals[65] and also for nonlinear optical crystal $LiNbO_3$.[66]

We did not apply this self-energy-correction scheme in the present calculation for TiO_2 since our main interest is in the comparison of electronic and optical properties of three phases of TiO_2. Most likely, the self-energy correction will lead to a rigid shift of the CB and a somewhat enlarged band gap. There will be no substantial changes in the LDA wave functions, and the calculated optical properties away from gap region should not be affected much. We can still expect the calculated static dielectric constants to be slightly reduced. Similar optical properties calculations on other oxides[67,68] actually show good agreement with experimental results in the high-energy region without the gap correction.

Our total-energy calculation for TiO_2 gives structural and elastic parameters in close agreement with the measured values and other theoretical calculations. We find

that the bulk modulus of anatase is larger than that of rutile by 30%, but that of brookite is substantially smaller. The elastic properties of anatase and brookite can be considered as theoretical predictions to be verified by future experiments. In particular, we have adopted a two-dimensional energy minimum search to determine the structural parameters of rutile. Our calculated c/a ratio and internal parameter are in excellent with experimental values.

The interband optical calculations produced results on the complex dielectric function, static dielectric constant, and energy-loss function for the three phases of TiO_2. All three phases show anisotropic structure in the dielectric function. For brookite, we predicted a much larger static dielectric constant than the other two phases. The good agreement between our calculation on the reflectance spectroscopy for rutile gives credence to results for the other two phases. This comprehensive study of three TiO_2 phases will be helpful for further investigations of the properties of defects, impurities, thin films, surfaces, and interfaces in the TiO_2 system.

ACKNOWLEDGMENT

This work was supported by the U.S. Department of Energy under Grant No. DE-FG02-84ER45170.

[1]M. F. Yan and W. W. Rhodes, in *Grain Boundaries in Semiconductors,* edited by H. J. Leamy, G. E. Pike, and C. H. Seager (North-Holland, New York, 1981).
[2]J. Reintjes and M. B. Schultz, J. Appl. Phys. **39**, 5254 (1968).
[3]J. B. Goodenough and J. M. Longo, in *Landolt-Börnstein Tabellen,* edited by K. H. Hellwege and A. M. Hellwege (Springer-Verlag, Berlin, 1970).
[4]S. J. Tauster, S. C. Fung, and R. L. Garten, J. Am. Chem. Soc. **100**, 170 (1978).
[5]D. J. Dwyer, S. D. Cameron, and J. Gland, Surf. Sci. **159**, 430 (1985).
[6]B. Poumellec, Ph.D. thesis, Université d'Orsay, 1986.
[7]A. Fujishima and K. Honda, Nature **238**, 37 (1972).
[8]R. I. Bickley, R. Soc. Chem. **5**, 308 (1982).
[9]R. H. Tait and R. V. Kasowski, Phys. Rev. B **20**, 5478 (1979).
[10]W. Göpel, J. A. Anderson, D. Frankel, M. Jaehnig, K. Phillips, J. A. Schäfer, and G. Rocker, Surf. Sci. **139**, 333 (1984).
[11]K. Tsutsumi, O. Aita, and K. Ichikawa, Phys. Rev. B **15**, 4638 (1977).
[12]A. F. Carley, P. R. Chalker, J. C. Riviere, and M. W. Roberts, J. Chem. Soc. Faraday Trans. **83**, 351 (1987).
[13]B. W. Veal and A. P. Paulikas, Phys. Rev. B **31**, 5399 (1985).
[14]R. Brydson, H. Sauer, W. Engel, J. M. Thomas, E. Zeitler, N. Kosugi, and H. Kuroda, J. Phys. Condens. Matter **1**, 797 (1989).
[15]L. A. Grunes, R. D. Leapman, C. N. Wilker, R. Hoffman, and A. B. Kunz, Phys. Rev. B **25**, 7157 (1982).
[16]M. L. Knotek and P. J. Feibelman, Phys. Rev. Lett. **49**, 964 (1978).
[17]B. Poumellec, P. J. Durham, and G. Y. Guo, J. Phys. Condens. Matter **3**, 8195 (1991).
[18]N. Daude, C. Gout, and L. Jouanin, Phys. Rev. B **15**, 3229 (1977).
[19]K. Vos, J. Phys. C **10**, 3917 (1977).
[20]L. B. Lin, S. D. Mo, and D. L. Lin, J. Phys. Chem. Solids **54**, 907 (1993).
[21]A. Hagfeldt, H. Siegbahn, S.-E. Lindquist, and S. Lunell, Int. J. Quantum Chem. **44**, 477 (1992).
[22]K. M. Glassford and J. R. Chelikowsky, Phys. Rev. B **46**, 1284 (1992).
[23]K. M. Glassford and J. R. Chelikowsky, Phys. Rev. B **47**, 12 550 (1993).
[24]D. Vogtenhuber, R. Podloucky, A. Neckel, S. G. Steinemann, and A. J. Freeman, Phys. Rev. B **49**, 2099 (1994).
[25]Shang-Di Mo, L. B. Lin, and D. L. Lin, J. Phys. Chem. Solids **55**, 1309 (1994).
[26]J. W. Halley, M. T. Michalewicz, and N. Tit, Phys. Rev. B **41**, 10 165 (1990).
[27]A. Fahmi, C. Minot, B. Silvi, and M. Causà, Phys. Rev. B **47**, 11 717 (1993).
[28]J. K. Burdett, T. Hughbanks, G. J. Miller, J. W. Richardson, Jr., and J. V. Smith, J. Am. Chem. Soc. **109**, 3639 (1987).
[29]P. Triggs, Helv. Phys. Acta **58**, 657 (1985).
[30]C. Gutiérrez and P. Salvador, J. Electroanal. Chem. **187**, 139 (1985).
[31]H. Berger, H. Tang, and F. Lévy, J. Cryst. Growth **130**, 108 (1993).
[32]M. Grätzel, Comments Inorg. Chem. **12**, 13 (1991).
[33]H. P. Maruska and A. K. Ghosh, Sol. Energy **20**, 443 (1978).
[34]H. Tang, K. Prasad, R. Sanjinés, P. E. Schmid, and F. Lévy, J. Appl. Phys. **75**, 2042 (1994).
[35]W. Y. Ching, J. Am. Ceram. Soc. **73**, 3135 (1990).
[36]E. Wigner, Phys. Rev. **46**, 1002 (1934).
[37]See, for example, G. Lehmann and M. Taut, Phys. Status Solidi **54**, 469 (1972).
[38]R. S. Mulliken, J. Am. Chem. Soc. **23**, 1833 (1955).
[39]F. D. Murnaghan, Proc. Natl. Acad. Sci. U.S.A. **30**, 244 (1944).
[40]D. T. Cromer and K. Herrington, J. Am. Chem. Soc. **77**, 4708 (1955).
[41]V. W. H. Baur, Acta Crystallogr. **14**, 214 (1961).
[42]J. Pascual, J. Camassel, and H. Mathieu, Phys. Rev. B **18**, 5606 (1978).
[43]P. I. Sorantin and K. Schwarz, Inorg. Chem. **31**, 567 (1992).
[44]K. C. Mishra, K. H. Johnson, and P. C. Schmidt, J. Phys. Chem. Solids **54**, 237 (1993).
[45]S. P. Kowlczyk, F. R. Mcfeely, L. Ley, V. T. Gritsyna, and D. A. Schirley, Solid State Commun. **23**, 161 (1977).
[46]H. Tang, H. Berger, P. E. Schmid, F. Lévy, and G. Burri, Solid State Commun. **87**, 847 (1993).
[47]R. Sanjinés, H. Tang, H. Berger, F. Gozzo, G. Margaritondo, and F. Lévy, J. Appl. Phys. **75**, 2945 (1994).
[48]M. H. Manghnani, J. Geophys. Res. **74**, 4317 (1969); M. H. Manghnani, E. S. Fisher, and W. S. Brower, Jr., J. Phys. Chem. Solids **33**, 2149 (1972).
[49]J. K. Burdett, Inorg. Chem. **24**, 2244 (1985).
[50]M. Cardona and G. Harbeke, Phys. Rev. **137**, A1467 (1965).
[51]K. Vos and H. J. Krusemeyer, J. Phys. C **10**, 3893 (1977).
[52]R. H. French, R. M. Canon, L. K. Denoyer, and Y.-M. Chiang, Solid State Ionics **75**, 13 (1995).
[53]S. H. Wemple, J. Chem. Phys. **67**, 2151 (1977).
[54]J. P. Perdew and M. Levy, Phys. Rev. Lett. **51**, 1884 (1983); L. J. Sham and M. Schluter, *ibid.* **51**, 1888 (1983).
[55]A. Zunger, J. P. Perdew, and G. L. Oliver, Solid State Com-

mun. **34**, 933 (1980); J. P. Perdew and A. Zunger, Phys. Rev. B **23**, 5048 (1981).
[56]R. A. Heaton, J. G. Harrison, and C. C. Lin, Solid State Commun. **41**, 827 (1982); R. A. Heaton and C. C. Lin, Phys. Rev. B **17**, 853 (1984).
[57]R. A. Heaton, J. G. Harrison, and C. C. Lin, Phys. Rev. B **28**, 5992 (1983).
[58]F. Gan, M.-Z. Huang, Y.-N. Xu, W. Y. Ching, and J. G. Harrison, Phys. Rev. B **45**, 8248 (1992).
[59]M. S. Hybertsen and S. G. Louie, Phys. Rev. B **34**, 5390 (1986); **37**, 2733 (1988).
[60]J. Q. Wang, Z. Q. Gu, and M. F. Li, Phys. Rev. B **44**, 8707 (1991).
[61]R. Hott, Phys. Rev. B **44**, 1057 (1991).
[62]A. Rubio, J. L. Corkill, M. L. Cohen, E. L. Shirley, and S. G. Louie, Phys. Rev. B **48**, 11 810 (1993).
[63]O. Zakharov, A. Rubio, X. Blase, M. L. Cohen, and S. G. Louie, Phys. Rev. B **50**, 10 780 (1994).
[64]P. A. Sterne and J. C. Inkson, J. Phys. C **17**, 1497 (1984).
[65]Zong-Quan Gu and W. Y. Ching, Phys. Rev. B **49**, 10 958 (1994).
[66]W. Y. Ching, Zong-Quan Gu, and Y.-N. Xu, Phys. Rev. B **50**, 1992 (1994).
[67]Y.-N. Xu and W. Y. Ching, Phys. Rev. B **43**, 4461 (1991); **44**, 11 048 (1994).
[68]W. Y. Ching and Y.-N. Xu, Phys. Rev. Lett. **65**, 895 (1990); R. H. French, S. J. Glass, F. S. Oguchi, Y.-N. Xu, and W. Y. Ching, Phys. Rev. B **49**, 5133 (1994).